Available online at www.sciencedirect.com
ScienceDirect
Journal of Molecular Catalysis A: Chemical 281 (2008) 230–236
JOURNAL OF MOLECULAR CATALYSIS A: CHEMICAL
www.elsevier.com/locate/molcata

Dynamics of hillocks formation during wet etching

M.P. Suárez, D.A. Mirabella, C.M. Aldao *

Institute of Materials Science and Technology (INTEMA), University of Mar del Plata and National Research Council (CONICET), Juan B. Justo 4302, B7608FDQ Mar del Plata, Argentina

Available online 19 August 2007

Abstract

Etch hillocks formation was studied experimentally and modeled using the Monte Carlo method. Simulations were used to explore the consequences of site-dependent detachment probabilities on surface morphology for a one- and two-dimensional substrate models. Comparison with pyramidal etch hillocks that are regularly observed in anisotropic etching of Si(1 0 0) are presented. The steady-state morphologies are analyzed and the hillock size distributions determined. The mechanisms responsible for the steady-state morphologies are described.
© 2007 Elsevier B.V. All rights reserved.

Keywords: Etching; Roughness and topography; Monte Carlo simulations; Scanning electron microscopy

1. Introduction

Anisotropic etching of silicon in aqueous solutions, such as KOH or NH_4OH, is widely used in producing a variety of devices by micromachining that requires the production of microstructures with nanometer precision. The formation of micropyramids that accompany Si(1 0 0) etching is a well-known phenomenon and an explanation for their appearance has been the objective of many investigations for years [1–6]. However, a basic understanding of the surface chemistry of the etch process is still controversial. There is consensus in that etch hillocks are not related to some surface condition or sample characteristic but hillocks are created during the etching process.

The presence of high-anisotropic dissolution ratios in silicon is very well known, with the (1 0 0) and (1 1 0) surfaces dissolving much more rapidly than the (1 1 1) plane [7,8]. This leads to exposing the slower etching (1 1 1) planes, which constitute the sides of pyramidal features. Furthermore, protruding shapes – like pyramidal hillocks – are expected to etch fast and then they should be unstable and prone to disappear. The formation of pyramids, then, implies not only strong (1 1 1) surfaces but also that their tops (apices) must etch slow. It has been suggested that some type of semipermeable or masking effects at the top of the pyramids make them stable. H_2-bubbles produced during the reaction, some reaction products, or some impurities present in the solution have been proposed to be responsible for affecting the etching rates at specific sites [9–13]. Other mechanisms, such as an etch-and-growth phenomenon and a self-stabilizing process have been also proposed [14]. So far, the explanation for this etching rate reduction continues being under debate [15]. In short, pyramids formation requires four conditions that must be satisfied: the existences of micromasking, relatively fast bottom surface etch rate, stable pyramid facets, and stable pyramid edges [16,17].

If etching at step and kink sites is much faster than at terraces and steps etch independently, step-flow etching predominates. This means that the crystal is etched by the continuous retreat of the steps. In this case, the surface morphology is dominated by step roughening since terraces are rarely attacked. Then, we only need to model and describe a one-dimensional substrate that represents a step. Etching in vicinal Si(1 1 1) surfaces has been found and described in this way [18–20]. The surface morphology can also be dominated by step bunching. This was considered to be due to inhomogeneities that develop in the etchant affecting local etch rates. We will not deal with step bunching in this work or, in general, with any complexity originated by diffusion. This has been considered to have a minor role in the formation of hillocks [17,21–23].

In this article we report experimental observations of Si(1 0 0) etching and Monte Carlo results for a one- and two-dimensional Kossel substrates extending our previous findings recently reported [24]. We explore and describe, within a site-dependent detachment probability model, the mechanisms responsible for hillock formation and their interrelation that contribute on the

* Corresponding author.
E-mail address: cmaldao@mdp.edu.ar (C.M. Aldao).

1381-1169/$ – see front matter © 2007 Elsevier B.V. All rights reserved.
doi:10.1016/j.molcata.2007.08.012

final surface morphology. In this context, we also discuss the effects of some factors that affect the hillock formation, including temperature, etchant concentration, etch agitation, and the presence of gases diluted in the solution.

Other authors have made important contributions related to modeling the resulting hillocks after wet etching in Si(1 0 0). For instance, Nijdam et al. studied the formation and stabilization of pyramids in great detail but they restrict the analysis to a single pyramid [9]. On the other hand, Gosálvez and Nieminen reproduced a complete surface texturization [16]. A main capability of our model is to reproduce the pyramid-and-valley patterns that regularly appear under steady-state etching, something not achieved with other models.

2. Experiments

Samples used in our studies were of n-type, P-doped, 4.5 Ω cm of resistivity, oriented within 0.5° of (1 0 0). Prior to the experiments, samples were chemically cleaned by immersion for 2 min in 2 M hydrofluoric acid to remove the native oxide layer. Samples were then rinsed in tetradistilled water. Studies were carried out with samples of about 1 cm × 1 cm in a glass cell.

Silicon wafers were supported horizontally in a Teflon holder within a Pyrex vessel mounted on a hot plate stirrer with controlled temperature to within ±1 °C. Wafers were etched in 0.5–6 M KOH solutions until steady state (2 h), after the etchant was allowed to reach the desired temperature, and then removed from the vessel, rinsed in cold tetradistilled water and dried in vacuum. The etched crystal surfaces were imaged with a scanning electron microscope (SEM). The specimen surfaces were not metal-coated prior to observation.

3. Simulation framework

We performed the simulation using the standard Monte Carlo method. The crystal surface is represented by a one (1D) or two (2D) dimensional matrix where each element corresponds to the height at the site describing the crystal surface. As stated above, we developed a model using a Kossel crystal that describes etching with a minimum of assumptions in a square lattice and in a simple cubic lattice.

The analysis is based on the so-called restricted solid-on-solid (RSOS) model in which particles are arranged such that the heights of neighboring columns can differ at most by only one particle [25]. The substrate configuration is then determined by the height of the columns relative to a flat reference surface. Sites are chosen at random and their neighborhoods are inspected in order to calculate the detachment probability of the surface particle. The detachment probability is related to the number of first neighbor bonds n needed to be broken to remove the particle, and then their energy E: $\exp(-nE/kT)$. Additional energy terms have been proposed [26]. However, we prefer to keep our model as simple as possible with only two parameters reflecting substrate strength and micromasking, which are enough to reproduce the experimentally observed morphologies.

During the simulation, single particles are randomly removed from the surface in accordance with predefined, site-specific etch rates. This is the only process that determines the final surface morphology. Other processes, such as rearrangement of surface particles (diffusion) or redeposition, are not allowed. The initial substrate configuration is flat but, since we are interested in the steady-state morphology, this is not relevant. The system evolves with successive annihilations of substrate particles until it approaches a steady-state configuration. We checked that steady state was reached by assessing the evolution of the surface roughness.

As stated above, we adopt the RSOS in order to take into account that the (1 1 1) surface dissolves much more slowly than the (1 0 0) one. Thus, since the RSOS prevents detachments from (1 1 1) surfaces, no chemical attack to particles in that crystallographic plane can take place in the model.

For hillocks to form, their tops must etch slower than one would expect from site-bonding energetics. This was taken into account by reducing the etching rate of apices that is by introducing micromasking. Thus, the surface morphology is controlled by the relative rates of site-specific etching that determine the annihilation probability of particles at different configurations. In short, the model allows for adjusting the interaction energy E between neighbors and the annihilation probability of apices. Monte Carlo simulations were carried out for a square lattice of 200 × 200 (2D surface) and for an array of 1000 sites (1D step). With these substrates, size effects are negligible. Periodic boundary conditions were used to avoid edge effects. Given our computational capabilities, we cannot perform an atomistic approach reproducing the surface morphology in its actual size. We focus here in mimicking the general features and trends experimentally observed.

4. Experimental results

Several factors affect the hillock formation, including temperature, etchant concentration, etch agitation, and the presence of gases. We found an important dispersion in the experimental results, very likely due to the high sensitivity on the different parameters involved. Anyway, general trends were detected in agreement with other authors [27]. Etch agitation, as well as ultrasonic bath, affects the hillock formation and, when strong enough, hillocks do not form.

Fig. 1 shows a SEM image of a Si(1 0 0) surface etched in 2 M KOH solution for 2 h at 60 °C (1 M is about 5.6 wt.% concentration). The surface exhibits a rough appearance with pyramidal hillocks of different sizes. The regions between hillocks are not flat but show smaller hillocks making a difficult task to determine their density because the counting depends on the instrument resolution. This etch surface, obtained under the above conditions, will be taken as the reference morphology.

Etchant concentration has a large effect on the resulting surface morphology. Fig. 1 shows that with a low KOH concentration the surface becomes very rough, the valleys seem to disappear, and the whole surface is covered with hillocks. Conversely, a high KOH concentration sharply reduces the hillock

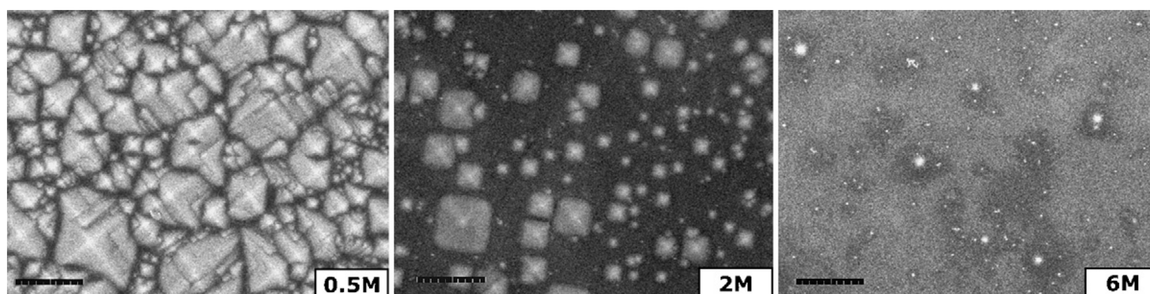

Fig. 1. Hillocks on a Si(1 0 0) surface etched in 0.5, 2, and 6 M KOH solutions during 2 h at 60 °C. The bar size is 10 μm (1 M is about 5.6 wt.% concentration).

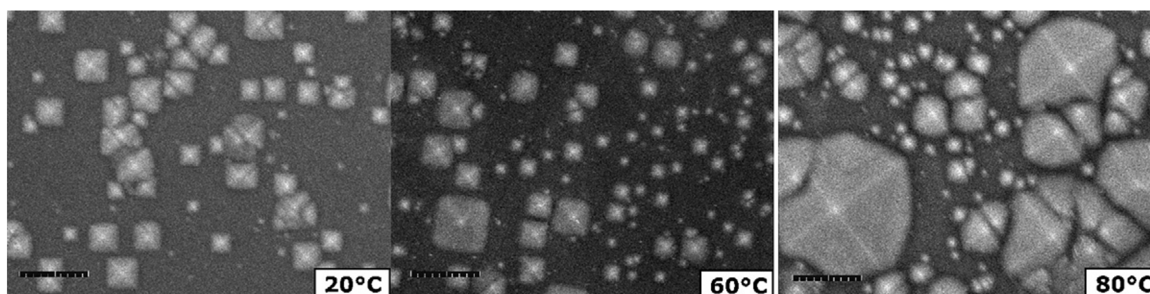

Fig. 2. Hillocks on a Si(1 0 0) surface etched in a 2 M KOH solution during 2 h at 20, 60 and 80 °C. The bar size is 10 μm.

formation. After etched in 6 M KOH, the surface shows isolated small hillocks.

Temperature also has a strong influence on the hillock formation (see Fig. 2). It is observed that the higher the temperature, the rougher the resulting surface. With temperature hillocks appear larger and the valleys seem to be much smaller. Also, with temperature, octagonal hillocks are more common.

Marked differences in surface morphology were obtained when the etchant is saturated with different gases [10,12,28,29]. In Fig. 3 the consequences of saturating the etch solution with argon, nitrogen, and oxygen are evident. Argon and specially nitrogen seem to facilitate the formation of hillocks while oxygen completely prevents their formation. These results can be due to the effects of these gases on the mask formation and stabilization and also on some effect on the substrate stiffness (see next section).

5. Computational results and discussion

In our model particles are removed (etched) from the surface accordingly with its site-specific etch rate taking into account only interactions to first neighbors. Thus, the parameters that determine step morphology reduce the etching rates of three distinct sites related to the particle coordination number. Since we are dealing with a solid-on-solid model, all particles have at least one first neighbor at the bottom that has no effect in computing the site-specific etch rates. Having this in mind, the etching rates will be referred as k_i, where i is the number of first neighbors excluding the bottom one: 0 for apices, 1 for kinks, and 2 for step sites (see Fig. 4). Since we are interested in the steady-state morphology, only the ratios between these parameters are relevant.

Monte Carlo simulations were performed for a variety of site-specific rate constants. We found that for hillocks to form not only relatively stable hillock apices are needed but also step sites must etch slowly [18]. Therefore, kinks must be the fastest etching sites and then a value of 1 was adopted for k_1. Step sites must be strong and we explored different values of k_2. To investigate the role of apex sites, in Fig. 5(a) we present etched profiles for several values of k_0 with $k_2 = 0.005$. It is observed that for $k_0 = 0.25$, the etched step morphology is relatively straight. As k_0 is decreased (apices becomes more stable), hillocks appear.

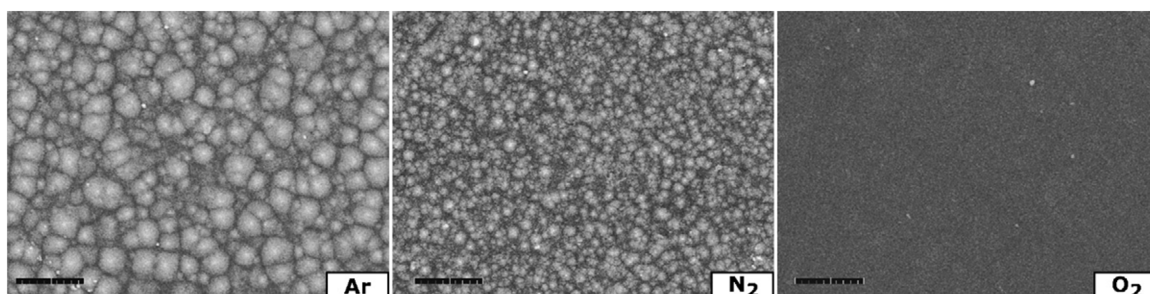

Fig. 3. Si(1 0 0) surface etched during 2 h in argon (Ar), nitrogen (N), and oxygen (O) saturated with 2 M KOH for 2 h. The bar size is 10 μm.

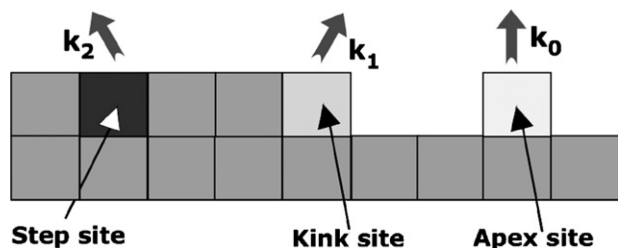

Fig. 4. Scheme of a one-dimensional substrate describing particles at the three possible sites defined by the number of first neighbors within a solid-on-solid model: apex, kink, and step sites. k_0, k_1, and k_2 are the etch rates corresponding to these sites.

For values of $k_0 \sim 0.1$, the surface presents hillocks separated by flat regions. As k_0 is decreased even further the hillocks are the prevailing feature because apices have a less probability to be removed, while etching continues at the valleys reducing their size to eventually make them disappear.

Fig. 5(b) shows the dependence of the surface morphology on k_2 for a fixed value of k_0. Note that a small value of k_2 represents a strong substrate. Thus, as expected, the surface becomes smoother as k_2 is reduced because hillocks are relatively more unstable.

Statistical analysis of the resulting morphologies is presented in Fig. 6 where the relative number of apices and the relative surface roughness are plotted as a function of k_0. The surface roughness, or interface width, is defined as

$$w = \sqrt{\frac{1}{L}\sum_{i=1}^{L}[h(i) - \bar{h}]^2},$$

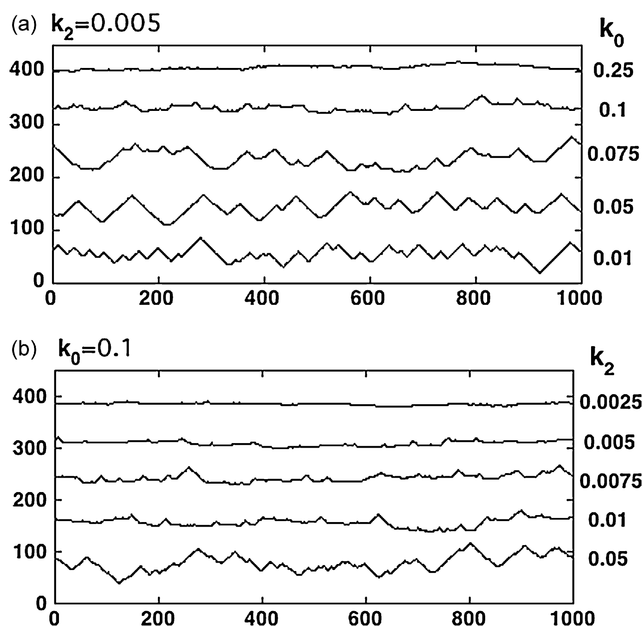

Fig. 5. (a) Simulated etch morphologies of a one-dimensional substrate with different etch rates for apex sites. The etching rate for kinks is $k_1 = 1$ and the etching rate for step sites is $k_2 = 0.005$. (b) Simulated etch morphologies of a one-dimensional substrate with different etch rates for step sites. The etching rate for kinks is $k_1 = 1$ and the etching rate for apices is $k_0 = 0.1$.

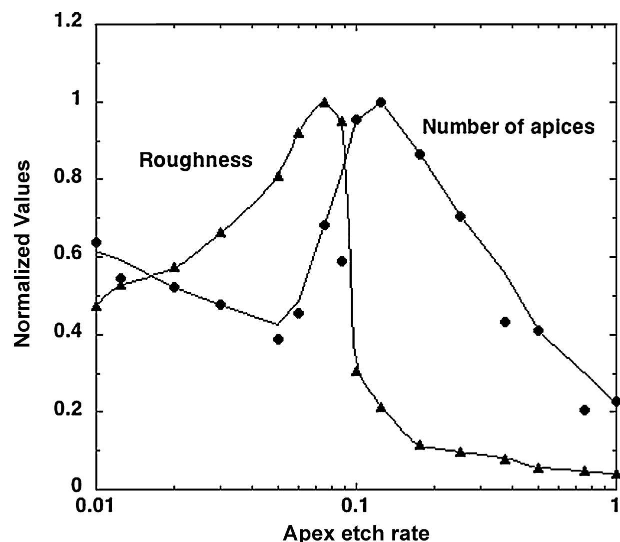

Fig. 6. Normalized number of apices and roughness as a function of apex etch rate for a one-dimensional substrate. Etching rates for kinks and step sites are $k_1 = 1$ and $k_2 = 0.005$, respectively.

where L is the number of sites, $h(i)$ the height of the column in site i, and $\bar{h}$ is the mean height of the surface. We will analyze now the effect of k_0 from large to small values (from $k_0 = 1$ to 0.01). For very large values of k_0 (>0.8) the number of apices and the roughness are low. As k_0 is reduced, the number of apices rapidly increases. Conversely, k_0 does not affect seriously the roughness because hillocks are very small for $k_0 > 0.2$. At this point hillocks start to increase considerably their size and the roughness is sharply affected. While the roughness increases, the number of apices decreases, that is consistent with a morphology presenting large hillocks. In the $0.1 < k_0 < 0.07$ range a hillock-and-valley morphology is observed. Further reduction of k_0 corresponds to a morphology in which there are no valleys, hillocks are smaller as k_0 is reduced, and then the roughness decreases. This is a direct consequence of the high-hillock stability; valleys continue being etched relatively fast and then they disappear.

We will focus next on the hillock-and-valley patterns that only form for a reduced range of k_0 and discuss how the number and size of the hillocks are a consequence of several non-simple interrelated mechanisms.

The etching rate of a valley directly depends on the density of kinks, as kink etching is a much faster process than etching at a step site. Kinks are created when particles at a step site are removed. Therefore, it is expected that the etching rate of a valley increase with its size as the number of available particles to be removed is larger and thus the formation of kinks is more likely. The rate at which a hillock is etched is dominated by k_0 since this is the limiting etching rate in this feature. k_0 is exactly the etching rate for a hillock of width one (formed by one particle). In larger hillocks, etching is more complicated because, once a hillock apex is removed, the top of the hillock has three particles; two of them are kink sites and one a step site. Eventually, two of these particles will be rapidly removed to end up with a new apex.

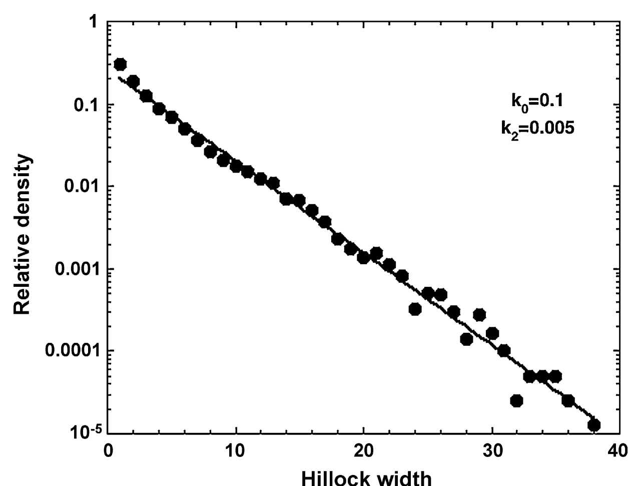

Fig. 7. Hillock size distribution for apex etch rate $k_0 = 0.1$ and step site rate $k_2 = 0.005$. Etching rate for kinks is $k_1 = 1$. The distribution can be very well fitted with a decreasing exponential. Distributions were obtained by averaging 1000 patterns after reaching steady state.

For an apex to form two opposing kinks must collide and thus a small hillock is created. This hillock can rapidly disappear if an etching event occurs for the only particle that constitutes the hillock. If the just formed apex remains stable while the surroundings are etched away, the hillock grows. If apex etching is too high, as soon as an apex forms it is etched and then the number of hillocks are very small. If apex etching is too low, hillocks grow to finally constitute the whole pattern.

At first glance, it seems that hillocks could adopt any size at random. However, Fig. 7 shows that the hillock size distribution for $k_0 = 0.1$ and $k_2 = 0.005$ has a distinct shape. Indeed, the distribution clearly presents an exponential-like form. Note that hillocks are continuously created and annihilated which is a consequence of hillock and valley etching. In steady state the creation and annihilation of hillocks must be equal. If a hillock is etched faster than the neighbor valleys, it shrinks. Conversely, if a hillock is etched slower than the neighbor valleys, it enlarges. The hillock size distribution following a decaying function indicates that hillock etching is in average faster than growing. The ratio between these etching rates is responsible for the average hillock size.

The described mechanisms are interconnected and they are responsible for the observed morphology. On one hand, the bounded valleys must have a width for which creation and annihilation of apexes is the same. On the other hand, the valley width determines the valley etch rate that together with the hillock etching rate are responsible for the hillock size distribution.

The discussions for one-dimensional substrates can be extended to explain the pyramid formation in two-dimensional substrates. Fig. 8 shows Monte Carlo simulations carried out for a square lattice of 200 × 200 sites. We considered that particles are etched away with a probability proportional to $\exp(-nE/kT)$. For a two-dimensional substrate, n refers to the number of first neighbors and E, as for a one-dimensional substrate, is attractive interaction energy.

The pyramid formation implies that apices are more stable than expected according to the number of neighbors. An extra parameter is then needed to lower the apex etch rate. Thus, we introduced the transparency factor $P < 1$ which represents a masking effect that reduces the etching of apices. Mathematically, the apex removal probability determined through $\exp(-nE/kT)$ is multiplied by a factor P reducing the etching rate since $P < 1$. We chose a value 10^{-3} for P because it is the masking that generates hillocks in the one-dimensional substrate [16]. Then, we found that $E/kT \sim 2.3$ produces the desired pyramid-and-valley morphology for a two-dimensional substrate.

Fig. 8(a) is the resulting surface corresponding to $E/kT = 2.3$ (i.e., a reducing factor in the etch probability of 0.1 per neighbor) and $P = 10^{-3}$. The surface morphology resembles that found in the experiments with pyramidal hillocks and valleys. Fig. 8 also shows the influence of E and P on the resulting surface morphology. As seen, the surface morphology is very sensitive to both parameters. Fig. 8(c) was obtained with $E/kT = 2.41$ and Fig. 8(b) with $E/kT = 2.21$. In this small range of the substrate strength, the morphology changes from having a few very small hillocks to big hillocks that cover most of the surface. Changes in P produce

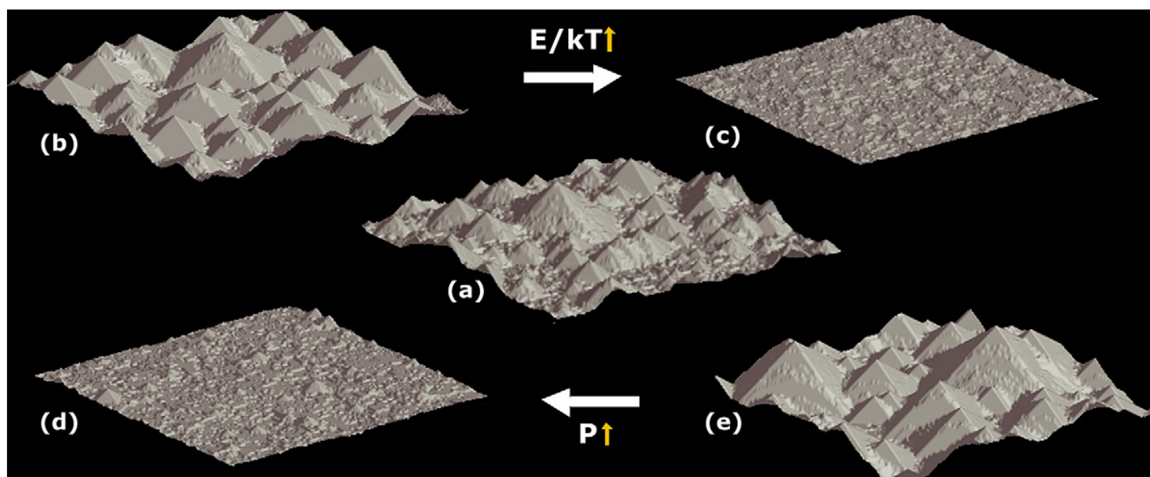

Fig. 8. Simulated etch morphologies of a two-dimensional substrate for (a) $E/kT = 2.3$ and $P = 10^{-3}$, (b) $E/kT = 2.21$ and $P = 10^{-3}$, (c) $E/kT = 2.41$ and $P = 10^{-3}$, (d) $E/kT = 2.3$ and $P = 1.4 \times 10^{-3}$, and (e) $E/kT = 2.3$ and $P = 5 \times 10^{-4}$. Smaller values of E and P make the surface to present larger hillocks that dominate the landscape.

similar effects than those of E. A smaller value of the transparency factor, see Fig. 8(e) for $P=5\times10^{-4}$, makes hillocks more stable and then they become larger and cover most of the surface. Conversely, a not much larger value of the transparency factor, see Fig. 8(d) for $P=1.4\times10^{-3}$, makes hillocks much smaller and thus the surface reduces radically its roughness.

We compare next the model outcomes with the experiments. In doing it, we only indicate general and qualitative trends. Experiments show that, regardless dispersion in the results, the hillock density and size increase with etching temperature and decrease with the KOH concentration [27]. Similar trends are observed in our model when E is decreased or P is increased.

The fact that the roughness decreases with etchant concentration seems to be counter-intuitive because one would expect that a faster etching involved a rougher surface. It is important to note that, under steady state, the ratios between the different etching rates determine the final surface morphology, not their absolute values. Gosálves and Nieminen [16] proposed that the origin of site-specific etching rates is due to the weakening of back-bonds that directly depends on the total number of OH attached to the atoms sharing the bond. A higher etchant concentration is expected to increase the differences in site-specific etching rates, since in average a higher number of OH will be attached to the surface atoms. Thus, to increase the etchant concentration would be equivalent to increase E in the model. As seen in Fig. 8, a larger value of E makes the roughness to decrease. A similar analysis can explain why a higher temperature results in a rougher surface; a higher temperature reduces the relative ratios between the etching rates.

It is found in the experiments that a large number of small hillocks appear when Ar and N are present. It has been proposed that nitrogen facilitates masking [11]. In our model, by reducing P, hillocks become more stable but this does not mean that they always become larger. This phenomenon already appears for one-dimensional substrates. Indeed, in Fig. 5(a) we can observe that for a very small value of k_0 (0.01) the surface presents a large number of small hillocks. Something similar occurs in two-dimensional substrates; this is observed in Fig. 9 where a surface with a large number of small hillocks forms for $P=2\times10^{-4}$. The resulting surface resembles the effect of gases such as Ar and N (see Fig. 3).

As commented in Section 1, Nijdam et al. [9] modeled the formation and fading away of a single pyramid. This is consistent

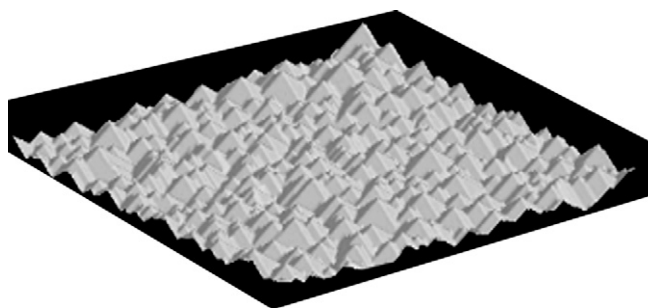

Fig. 9. Simulated etch morphology for a two-dimensional substrate for $E/kT=2.3$ and $P=2\times10^{-4}$. Very stable apices lead eventually to a surface covered with small hillocks.

with our results but this work does not focus on the wide surface morphology. Gosálvez et al. [17], on the other hand, include diffusion phenomena in order to explain the shallow round pits on (1 0 0) and the elongated zigzag structures on (1 1 0). Thus, diffusion only has an important role in the absence of micromasking, which is considered responsible for the pyramidal hillocks that appear on (1 0 0). Then, our work is also aligned with this hillock formation modeling.

As it can be seen from the above discussion, the idea of including masking is not new. However, the main advantage of our model is its simplicity that allowed a systematic study reproducing the general trends of the morphologies observed in the experiments by varying the model parameters. In doing this, we obtained the pyramid-and-valley patterns observed experimentally; we did not need to consider complexities of any other kind. Also, the analysis of the found patterns shed light on the formation and stabilization of the etching pyramids. We specially discussed how the number and size of the hillocks are a consequence of several non-simple interrelated mechanisms. As far as we know, none of the previous models successfully addressed these details. In particular, compared with ours, the model of Gosálvez and co-workers incorporate a more complex structure and more sophisticated removal rules, but their results only show a complete texturization (hillocks completely cover the surface).

As a final comment, we would like to emphasize that in the present model the masking acts exclusively on apices leading to a site-dependent etching rate model. Other complexities could be added, but we were looking here for the most basic and simple mechanisms that produce hillock-and-valley patterns [30]. We have performed other simulations in which masks are activated independently of the substrate site configuration but we were unable to reproduce this type of patterns. Despite its simplicity, the site-dependent etching model presents a very complex behavior and reproduces the main features experimentally observed.

6. Conclusion

A simple etching model, in which the only process present is the removal of particles, can show the formation of complex surface patterns. The model has only two parameters that represent the substrate strength and the micromasking effect. The formation of hillocks, a regular finding in Si(1 0 0) etching, can be reproduced. In particular, the experimentally observed pyramid-and-valley pattern under steady state is reproduced. The model indicates that this morphology appears to be governed by several interrelated phenomena. The effects of temperature, etchant concentration, etch agitation, and the presence of gases are interpreted within the general trends that the model predicts.

Acknowledgments

This work was partially supported by the CONICET (Argentina) and the ANPCyT (Grant No. 12-12561, Argentina). We are grateful to Héctor Asencio for his technical assistance.

References

[1] M. Elwenspoek, H. Jansen, Silicon Micromachining, Cambridge University Press, Cambridge, 1998.
[2] H. Seidel, L. Csepregi, A. Heuberger, H. Baumgärtel, J. Electrochem. Soc. 137 (1990) 3612.
[3] C.R. Tellier, A. Brahim-Bounab, J. Mater. Sci. 29 (1994) 5953.
[4] I. Zubel, I. Barycka, Sens. Actuator A 70 (1998) 250.
[5] Y. Jiang, Q. Huang, Semicond. Sci. Technol. 20 (2005) 524.
[6] D. Cheng, M.A. Gosálves, T. Hori, K. Sato, M. Shikida, Sens. Actuator A 125 (2006) 415.
[7] D.B. Lee, J. App. Phys. 40 (1969) 4569.
[8] R.A. Wind, M.A. Hines, Surf. Sci. 460 (2000) 21.
[9] A.J. Nijdam, E. van Veenendaal, H.M. Cuppen, J. van Suchtelen, M.L. Reed, J.G.E. Gardeniers, W.J.P. van Enckevort, E. Vlieg, M. Elwenspoek, J. App. Phys. 89 (2001) 4113.
[10] S.A. Campbell, K. Cooper, L. Dixon, R. Earwaker, S.N. Port, D.J. Schiffrin, J. Micromech. Microeng. 5 (1995) 209.
[11] T. Baum, J. Satherley, D.J. Schiffrin, Langmuir 14 (1998) 2925.
[12] T. Baum, D.J. Schiffrin, J. Micromech. Microeng. 7 (1997) 338.
[13] J. Chen, L. Liu, Z. Li, Z. Tan, Q. Jiang, H. Fang, Y. Xu, Y. Liu, Sens. Actuator A 96 (2002) 152.
[14] H. Schröder, E. Obermeier, A. Steckenborn, J. Micromech. Microeng. 9 (1999) 139.
[15] E. van Veenendaal, K. Sato, M. Shikida, A.J. Nijdam, J. van Suchtelen, Sens. Actuator A 93 (2001) 232.
[16] M.A. Gosálves, R.M. Nieminen, New J. Phys. 5 (2003) 100.
[17] M.A. Gosálves, K. Sato, A.S. Foster, R.M. Nieminen, H. Tanaka, J. Micromech. Microeng. 17 (2007) S1.
[18] J. Flidr, Y. Huang, M.A. Hines, J. Chem. Phys. 111 (1999) 6970.
[19] J. Flidr, Y. Huang, T.A. Newton, M.A. Hines, J. Chem. Phys. 108 (1998) 5542.
[20] T.A. Newton, Y. Huang, L.A. Lepak, M.A. Hines, J. Chem. Phys. 111 (1999) 9125.
[21] S.P. García, H. Bo, M.A. Hines, Phys. Rev. Lett. 93 (2004) 166102.
[22] S.P. García, H. Bo, M.A. Hines, J. Phys. Chem. B 108 (2004) 6062.
[23] M.A. Gosálves, Y. Xing, T. Hynninen, M. Uwaha, A.S. Foster, R.M. Nieminen, K. Sato, J. Micromech. Microeng. 17 (2007) S27.
[24] M.P. Suárez, D.A. Mirabella, C.M. Aldao, Surf. Sci. 599 (2005) 221.
[25] A.-L. Barabási, H.E. Stanley, Fractal Concepts in Surface Growth, Cambridge University Press, Cambridge, 1995.
[26] M.A. Gosálves, A.S. Foster, R.M. Nieminen, Europhys. Lett. 60 (2002) 467.
[27] S. Tan, M.L. Reed, H. Han, R. Boudreau, J. Microelectromech. Syst. 5 (1996) 1057.
[28] S.P. García, H. Bo, M. Manimaran, M.A. Hines, J. Phys. Chem. B 106 (2002) 8258.
[29] M.A. Hines, Annu. Rev. Phys. Chem. 54 (2003) 29.
[30] Z. Elalamy, L.M. Landsberger, A. Pandy, M. Kahrizi, I. Stateikina, S. Michel, J. Vac. Sci. Technol. A 20 (6) (2002) 1927.